

# Charge inversion, condensation and decondensation of DNA and polystyrene sulfonate by polyethylenimine<sup>\*</sup>

V. Mengarelli<sup>1,2</sup>, L. Auvray<sup>2,3</sup>, D. Pastré<sup>4</sup>, and M. Zeghal<sup>1,a</sup>

<sup>1</sup> Laboratoire de Physique des Solides, UMR CNRS 8502, Bât. 510, Université Paris-sud, 91405 Orsay, France

<sup>2</sup> Équipe Matériaux Polymères aux Interfaces, Université d'Évry, 91025 Évry, France

<sup>3</sup> Laboratoire Matière et Systèmes Complexes, CNRS-UMR7057, Université Paris 7, 75205 Paris, France

<sup>4</sup> SABNP, Inserm U829, Université d'Évry, 91025 Évry, France

Received 7 July 2011

Published online: 25 November 2011 – © EDP Sciences / Società Italiana di Fisica / Springer-Verlag 2011

**Abstract.** We study the formation and structure of stable electrostatic complexes between polyanions (DNA and poly(styrene-sulfonate)) and linear polyethylenimine. The charge ratio  $x$  of the mixture is tuned by varying the concentration of the polycation at constant concentration of polyanion. In agreement with recent theories, dynamic light scattering and electrophoretic mobility measurements show two distinct regimes of weak and strong complexation. At low polycation concentration, negatively charged small complexes involving a few polyanion chains are observed first. By further increasing  $x$ , these small complexes condense at a precise charge ratio  $x_c < 1$  to form large anionic aggregates. The inversion of the charge of the condensed complexes coincides with the maximum of complexation and precedes the dissolution of the aggregates which occurs at a well-defined decondensation threshold  $x_d > 1$ . Above  $x_d$ , positively charged complexes containing again a few overcharged polyanion chains are observed. The macroscopic phase diagram is qualitatively well corroborated by AFM observation of the complexes. The influence of entropic effects is probed by varying parameters like concentration, polycation molecular weight and ionic strength. Structure of stable negatively charged complexes is investigated at higher concentration using Small Angle Neutron Scattering. In the condensed regime, we observe large soluble bundles with sharp interfaces where the local structure of the polyanions is preserved.

## 1 Introduction

The deviation from electroneutrality in chemical systems by dissociation or association of molecules or ions is only possible if the macroscopic charging electrostatic energy is compensated by other contributions, mainly the entropic one in the case of ionic dissociation or binding energy in the case of association. In ionic systems at room temperature (when quantum effects are not relevant), this binding energy, for instance the famous Madelung energy of ionic crystals, is itself of electrostatic origin: interacting charges of opposite sign organize themselves locally to minimize the electrostatic energy. As recognized by several authors [1–3], this may lead to the interesting situation where the local binding part of the electrostatic energy competes with its long-range macroscopic part. Depend-

ing on cases, the final electrical charge of the system may be of either sign. In particular, binding cationic species to an anionic object may lead to a positively charged assembly: this is the phenomenon of “charge inversion” [4–6].

Charge inversion was observed by several authors in mixtures of charged polyelectrolytes with oppositely charged oligomers [7, 8], polymers [9–16], colloids [11, 17–20] or micelles [21] and has important applications. At surfaces, it enables the building of polyelectrolyte multilayers [22, 23]. It plays also an important role in gene transfer techniques, where polycations are used to condense, protect and invert the charge of DNA molecules favoring their merging with negatively charged cell membranes [9, 13, 24–26]. All these systems are strongly correlated, the electrostatic interactions are strong and the effects of thermal motions, translational or conformational entropy of chains small. This makes their theoretical description very difficult. In particular, simple mean-field theories cannot be used, since the effects of charges of opposite sign cancel at the mean-field level in neutral and uniform systems. Electrostatic binding, charge inver-

<sup>\*</sup> Supplementary material in the form of a PDF file available from the Journal web page at

<http://dx.doi.org/10.1140/epje/i2011-11127-3>

<sup>a</sup> e-mail: [zeghal@lps.u-psud.fr](mailto:zeghal@lps.u-psud.fr)

sion and their consequences on the structure and phase behavior of the systems are only described by taking into account the fluctuations of concentrations of the constituents and their correlations. In polymer systems, this is done by using the well-known “Random Phase Approximation” or other sophisticated theoretical methods [27, 28]. Numerical simulations are also very useful [29–33].

Recently, a simplified but illuminating analytical description of the formation of complexes of polyelectrolytes was given T.T. Nguyen, I. Rouzina and B. Shklovskii in terms of the electrostatic interaction between dilute polyanions and small multivalent polycations [1]. This approach was extended to complexes between long polyanions and short polycations [2, 3]. In the latter system, the Coulomb interactions are assumed sufficiently strong so that the entropy of the chains becomes negligible. In the absence of added salt, the only thermodynamic variable is the charge ratio  $x = Q^+/Q^-$  of the mixture, where  $Q^+$  ( $Q^-$ ) is the total charge of complexed and free polycations (polyanions) in solution. When  $x$  is far away from 1, complexes are strongly charged, negatively if  $x \ll 1$  or positively if  $x \gg 1$  (regime of charge inversion). In either case, short polycations are adsorbed on individual chains of polyanions, forming what one may call “binary” or “free” complexes, with a given electrostatic binding energy  $nE(n)$ , which depends on the number  $n$  of polycations per polyanion, ( $E(n)$  is the binding energy per polycation), and a given Coulomb self-energy, fixed by the overall charge and shape (capacitance) of one complex. Close to the point of neutralization ( $x = 1$ ), binary complexes condense, because this diminishes further the local electrostatic binding energy via local correlated rearrangements of the ions, and because the macroscopic Coulomb energy vanishes. By comparing the free energy of the different types of complexes, R. Zhang and B. Shklovskii show that binary complexes may coexist with condensed complexes. There are in fact two possibilities, either an inter-complex coexistence where a macroscopic neutral drop coexists with dilute charged binary complexes, or an intra-complex coexistence where free complexes rearrange themselves into a “tadpole” structure with a condensed neutral head and a strongly charged tail [2, 3]. By increasing  $x$ , one thus expects to observe successively a phase of stable negatively charged complexes, a phase separation occurring at a given condensation threshold  $x_c$  (depending on added salt) and a re-entrant phase of stable positively charged complexes, appearing above a well-defined decondensation threshold  $x_d$ ,  $x_c$  and  $x_d$  being symmetrically located on each side of the isoelectric point,  $x = 1$ . This approach describes the phenomenon of like charge attraction and charge inversion as purely electrostatic and mainly ruled by short-range correlations. Within this framework, the entropic nature of association [4, 34] due to the release of counterions is itself driven by correlations [5].

Experimentally, condensation of DNA and flexible polyelectrolytes can refer specifically to the collapse of individual long polymer chains into globular states [35, 36] or to the secondary aggregation of existing binary com-

plexes [7, 37, 38]. To our knowledge, the phase diagram described above has been observed alone [37] or accompanied by the charge reversal [7] only with mixtures of polyanions and small multivalent cations. In order to probe and generalize these ideas to polyelectrolytes, we have extended the study to the formation and structure of different linear polyanion-polycation complexes in the dilute regime. We use two polyanions, DNA and poly(styrenesulfonate)(PSSNa) of similar structural electric charge. The DNA molecules are short stiff monodisperse nucleosomal DNA fragments containing 146 base pairs corresponding to one persistence length,  $l_p = 50$  nm [39]. The utilization of more flexible PSSNa which has a ten times lower persistence length,  $l_p = 5$  nm, allows to probe the effect of the rigidity of the polyanion. Following the pioneering work of J.P. Behr and coworkers, Linear Polyethylenimine (LPEI) has become one of the most investigated condensing agents used in gene transfer and gene therapy techniques [13, 24, 25]. This is why our choice has focused on LPEI with two different molecular weights (25 kDa and 2.5 kDa). Most of DNA-PEI complexation studies deal with long plasmid DNA and PEI of different molecular weight. Condensation and overcharging of plasmid DNA by LPEI were reported [13, 25], but without mentioning the existence of (de)condensation thresholds. This is likely due to the use of long DNA molecules and low ionic strength conditions which can favor the formation of kinetically trapped and non-equilibrium assemblies. For that reason, we decided to study the complexation of short polyelectrolytes in the very dilute regime and at high ionic strength. We succeeded in obtaining stable complexes in the whole range of charge ratio and we measured their size and the electrophoretic mobility. We have also investigated the effect of polyanion stiffness, the polycation length, and the ionic strength on the phase diagram. The very same behavior is observed in all systems, whose qualitative features are well described by the theory of Zhang and Shklovskii. However, entropic effects, neglected in the theory, smooth the observed phase behavior.

Unfortunately, descriptions of the structure of soluble complexes at different scales in both anionic and cationic regimes are rare, especially for complexes of flexible polyelectrolytes [14, 15]. Infrared and circular dichroism revealed that the local B form of DNA is not affected by complexation with PEI [13]. Fluorescence microscopy studies of long DNA-multivalent ions have shown the coexistence between binary and condensed individual DNA strand complexes [35]. AFM studies of positively charged DNA-PEI complexes allowed to show that plasmids condense into bundled, folded loops of DNA, suggesting that most condensation proceeds through folding rather than winding DNA [36]. These AFM studies are transposed to our DNA-PEI complexes. Classical X-ray and neutron diffraction techniques which allow to probe the structure of polymers over a wide range of length scales are not convenient with such dilute systems. However, we also report Small Angle Neutron Scattering (SANS) experiments performed on both polyanions complexed with short and long PEI at higher concentration in the anionic regime.

## 2 Materials and methods

### 2.1 Sample preparation

DNA fragments were prepared from calf thymus as described by J.L. Sikorav *et al.* [39]. Chromatin was extracted in low ionic strength buffer. After removal of linker histones, 146 bp DNA was obtained by controlled digestion with micrococcal nuclease. After precipitation in cold 2-ethanol, DNA pellets were dried under vacuum and conserved at  $-80^{\circ}\text{C}$ . The pellets were solubilized in an adequate buffer—10 mM Tris—with the pH adjusted to 7.4 before using them. DNA concentrations were determined by UV absorption at 260 nm. The UV absorbances at 280 nm were also measured to determine the purities of the samples. The length of the fragments was determined by electrophoresis on agarose gels.

The Sodium poly(Styrene Sulfonate) (PSSNa,  $M_w = 77\text{ kDa}$ , polydispersity index:  $I = M_w/M_n = 1.1$ , where  $M_w$  ( $M_n$ ) refers to the weight (number) average of the polymer molecular weight) and linear polyethylenimine (LPEI,  $M_w = 2.5\text{ kDa}$  and  $25\text{ kDa}$ ,  $I = M_w/M_n = 2.5$  [40]) are provided respectively by Fluka and Aldrich. The stock PSSNa and LPEI solutions were prepared in the same buffer—purified deuterated water (Eurisotop) 10 mM Tris—and the pH was adjusted when needed to the value of 7.4 using a concentrated solution of DCl ( $[\text{DCl}] = 7.6\text{ M}$ ). In the case of the basic LPEI, the final ionic strength of the solution at  $\text{pH} = 7.4$  was  $[I] = 0.15\text{ M}$ . As a consequence, most of experiments were performed at this ionic strength. The electric charge of LPEI is obtained from independent titration experiments. We find:  $Q_{\text{LPEI } 2.5\text{ kDa}} = 13e$  and  $Q_{\text{LPEI } 25\text{ kDa}} = 130e$ . The structural charges of the DNA and PSSNa molecules are equal to  $Q_{\text{DNA}} = -300e$  and  $Q_{\text{PSSNa}} = -373e$ .

The charge ratio  $x = Q^+/Q^-$  of the complex is varied by increasing the mixing ratio of stock solutions of polyanion and polycation. The order of mixing is always the same: the complementary buffer volume necessary to adjust the final volume of the sample is first added to the polyanion stock solution. The polycation is added subsequently. Higher ionic strength complexes ( $[I] = 0.25\text{ M}$  and  $[I] = 0.65\text{ M}$ ) were obtained by adding first the required volume of NaCl ( $[\text{NaCl}] = 5\text{ M}$ ) to the polyanion.

### 2.2 Experimental methods

#### 2.2.1 Dynamic light scattering and electrophoretic mobility measurements

The dynamic light scattering (DLS) and electrophoretic measurements were performed using a “Malvern Zeta Potential Nano Sizer” operating at  $\lambda = 633\text{ nm}$  wavelength. The scattering vector  $q$  is defined as  $q = (4\pi n/\lambda) \sin \theta/2$ , with  $n$  the refractive index of the solvent and  $\theta$  the scattering angle.

In Dynamic Light Scattering, the normalized first-order electric field  $E(t, q)$  time correlation  $g^{(2)}(t, q)$  function is related to the time-intensity correlation function

through the Siegert equation [41].  $g^{(2)}(t, q)$  is related to the measured relaxation rate,  $\Gamma$ , according to

$$\langle E(t, q)E^*(t, q) \rangle = g^{(2)}(t, q) = \int_0^\infty G(\Gamma)e^{-\Gamma t} d\Gamma.$$

The autocorrelation function was analyzed in terms of continuous distribution of relaxation times  $\Gamma$  using the first cumulant method and/or CONTIN algorithm. The decay time  $\Gamma$  is related to the translational diffusion coefficient via  $\Gamma = Dq^2$ . The measurements were performed at the scattering angle of  $173^{\circ}$  and  $90^{\circ}$ . Using a smaller scattering angle could make the measurements more accurate, but it will not significantly affect the trends of the results. The relation between the diffusion coefficient  $D$  and the frictional or drag coefficient is given by Einstein's relation

$$D = k_B T / f. \quad (1)$$

For a complex in a solvent of viscosity  $\eta$ , the drag coefficient  $f$  is related to the hydrodynamics radius  $R_h$  of the equivalent Stokes sphere by the Stokes relation  $f = 6\pi\eta R_h$ . For bare mononucleosomal DNA, assimilated to a rigid rod of length  $L$  and radius  $d = 20.1\text{ \AA}$  [42], the friction coefficient is given by ( $p = L/d$ ) [42, 43]

$$f = 3\pi\eta L / \ln(p) + 0.312 + \frac{0.565}{p} - \frac{0.1}{p^2}. \quad (2)$$

Electrophoretic mobility measurements based on the laser doppler velocimetry principle yields the velocity of the complexes submitted to an alternating electrical field of  $125\text{ V/cm}$  oscillating at a frequency of  $20\text{ Hz}$ . Therefore, the recorded frequency shift is directly related to the velocity of complexed DNA. The independent measurements of  $\mu$  at low electric field and  $D$  are related to the electrophoretic effective charge  $Q_\mu$  according to the Nernst-Einstein equation

$$Q_\mu = \mu f = \frac{\mu k_B T}{D}. \quad (3)$$

This definition of the charge is almost always lower than the real charge due to the retarding influences of the counterion cloud [44–46].

Unless stated otherwise, measurements were done at low polyanion concentration of  $0.01\%$  ( $w/v$ ), ionic strength  $[I] = 0.15\text{ M}$  and  $\text{pH} = 7.4$ . All measurements were performed at  $20^{\circ}\text{C}$  ( $\eta = 10^{-3}\text{ Pa s}$ ), 24 hours after sample preparation and repeated one month later in order to check the stability over time of the characteristics of the complexes. It is important to mention that for all charge ratios, the concentration of free polycations is too low to produce any significant contribution to the DLS signal or to the frequency shift spectrum during electrophoretic mobility measurements.

#### 2.2.2 AFM imaging

AFM imaging was performed in Tapping Mode TM with a MultimodeTM AFM (Veeco, Santa Barbara, CA) operating with a Nanoscope IIIaTM controller. We used Olympus (Hamburg, Germany) silicon cantilevers AC160TS

with nominal spring constants between 36 and 75 N/m. The scan frequency was typically 1.5 Hz per line and the modulation amplitude was a few nanometers. The DNA/LPEI complexes were diluted to a concentration of 0.01% (DNA) in a buffer solution containing (MgCl<sub>2</sub> 5 mM, pH 7.4). A 5  $\mu$ l droplet was deposited onto the surface of freshly cleaved mica (muscovite) for 1 min. Then, the surface was rinsed with 0.02% diluted uranyl acetate solution in order to stabilize complexes in their 3D conformations for AFM imaging in air. The sample was then rapidly rinsed with pure water (Millipore) to obtain a clean surface after drying with filter paper. The use of uranyl acetate discriminates between weak and firmly adsorbed molecules [47].

### 2.2.3 SANS measurements

The small angle neutron scattering experiments were performed at Laboratoire Léon Brillouin (Saclay, France) on the PACE spectrometer on a  $q$  range lying between  $4 \cdot 10^{-3}$  and  $2 \cdot 10^{-1} \text{ \AA}^{-1}$ . Standard corrections for sample volume, neutron beam transmission, empty cell signal subtraction, and detector efficiency have been applied to get the scattered intensities on an absolute scale. The polyanion concentration in D<sub>2</sub>O is 0.2% ( $w/v$ ), in order to ensure a measurable intensity. The samples were prepared as described above and the final ionic strength of the solution at pH = 7.4 was  $[I] = 0.15 \text{ M}$ . Measurements were performed on soluble and stable complexes 24 hours after sample preparation.

## 3 Results and discussions

### 3.1 Diffusion and electrophoretic mobility of 146 bp DNA

In order to characterize the mononucleosomal DNA, DLS and electrophoretic measurements were carried out at very low concentration ( $c = 0.005\%$ ) and sufficiently high ionic strength ( $I = 0.15 \text{ M}$ ). Diffusion light scattering measurements performed on similar short monodisperse DNA fragments at higher concentration have shown fast and slow relaxation modes [42, 48]. At sufficiently high ionic strength and low concentration,  $g^{(2)}(t, q)$  functions present only the fast mode. This fast mode allowed to extract the value of the translational self-diffusion coefficient  $D$  which is found to be independent of the scattering vector  $q$ . The  $g^{(2)}(t, q)$  function measured with our 146 bp DNA shows one relaxation mode yielding an apparent diffusion coefficient  $D = 3.36 \cdot 10^{-7} \text{ cm}^2 \text{ s}^{-1}$ . This value combined with eqs. (1) and (2) yield a DNA length  $L = 44 \text{ nm}$ , slightly lower than the 146 bp DNA length of 50 nm. Our experimental values of  $D$  and  $L$  are close to those reported for double strand 160 base pair DNA ( $D = 3.1 \cdot 10^{-7} \text{ cm}^2 \text{ s}^{-1}$ ) [48].

The electrophoretic mobility is independent of DNA molecular weight above ca. 170 bp. Below this threshold corresponding to about one persistence length, the mobility decreases monotonically with decreasing molecular

weight for smaller fragments [46, 49]. Furthermore, electrophoretic measurements across a range of ionic strength show that DNA mobility is drastically reduced upon salt addition [44]. In our case, the electrophoretic mobility of bare DNA is found to be  $\mu = -2 \cdot 10^{-4} \text{ cm}^2 \text{ s}^{-1}$ , a value lower in absolute value than that obtained without added salt, but close to that one reported for long duplex DNA at higher ionic strength [44]. The values of  $D$ ,  $\mu$  and eq. (3) yield a DNA electrophoretic effective charge  $Q_{\mu}^{\text{DNA}} = -17e$ . As expected, at high ionic strength,  $Q_{\mu}^{\text{DNA}}$  is much lower than the DNA charge partially compensated by Manning's condensation  $Q_m^{\text{DNA}} \simeq -70e$ .

### 3.2 Phase diagram of the complexes

The variations at constant polyanion concentration of the hydrodynamics radius  $R_h$  and electrophoretic mobility  $\mu$  of the DNA/LPEI-2.5 kDa and PSSNa/LPEI-2.5 kDa complexes with the charge ratio  $x = Q^+/Q^-$  are shown in fig. 1. The formation of complexes, their condensation and decondensation associated with their charge inversion are manifest. By increasing  $x$ , we first observe a small increase of the hydrodynamic radius followed by a large growth occurring for  $x$  close to 1 and a decrease when  $x$  becomes larger than 1. The complexes are negatively charged ( $\mu < 0$ ) when  $x \ll 1$  and positively charged for  $x \gg 1$ . The charge inversion ( $\mu = 0$ ) occurs at  $x = 0.83$  for DNA and at  $x = 0.65$  for PSSNa. It coincides in both cases with the maximum of complexation. The diffusion coefficient  $D = 0.54 \cdot 10^{-7} \text{ cm}^2 \text{ s}^{-1}$  of DNA complexes at small  $x$  is much lower than that of the bare DNA. Hence, the corresponding hydrodynamics radius  $R_h = 40 \text{ nm}$  of the complexes is too large to be only due to the adsorption of small 2.5 kDa PEI molecules on DNA strands. This suggests that DNA strands are already slightly aggregated and form small primary complexes. In order to confirm this point, we estimate the electrophoretic effective charge  $Q_{\mu}^c$  of one complex from eq. (3). For  $x = 0.44$  ( $D = 0.46 \cdot 10^{-7} \text{ cm}^2 \text{ s}^{-1}$ ,  $\mu = -2.2 \cdot 10^{-4} \text{ cm}^2 \text{ V}^{-1} \text{ s}^{-1}$ ), one obtains  $Q_{\mu}^c = -120e$ , a much higher value than the electrophoretic charge of the bare DNA molecules in the condition of the experiments ( $Q_{\mu}^{\text{DNA}} = -17e$ ). One cannot in principle directly compare the electrophoretic charges of the complex and of the bare DNA because of the complex interplay between the electric, hydrodynamic and electro-osmotic forces in polyelectrolytes systems [44, 45, 50, 51], but the difference of values is large enough to demonstrate primary complexation. It is also interesting to evaluate the effective charges of the complexes  $Q_m^c$ , given by  $Q_m^c = Q_m^{\text{DNA}}(1 - x)$ . It is assumed that one complex contains only one DNA molecule and that a fraction  $x$  of the bare charges is fully neutralized by PEI while the remaining fraction  $(1 - x)$  is partially compensated by Manning's condensation of the counterions. For  $x = 0.44$ ,  $Q_m^c = -40e$ . If we assume one DNA per complex, we obtain that the effective charge is smaller (in absolute value) than the electrophoretic charge, which is not possible. We again conclude that the observed complexes must be aggregated with several DNA chains per complex. A number

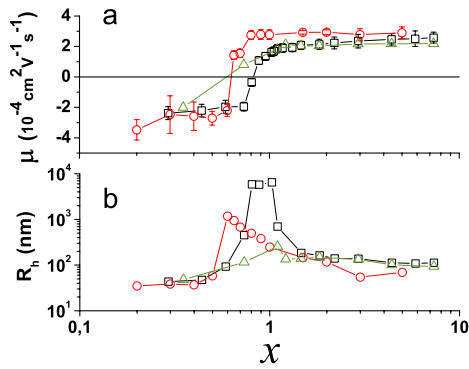


**Fig. 1.** Electrophoretic mobility (a) and hydrodynamics radius (b) plotted as a function of the charge ratio  $x$ . Polyanion concentration  $c = 0.01\%$  ( $w/v$ ),  $[I] = 0.15$  M,  $pH = 7.4$ : DNA/LPEI-2.5 kDa complex ( $\square$ ), PSSNa/LPEI-2.5 kDa complex ( $\circ$ ). Polyanion concentration  $c = 0.005\%$  ( $w/v$ ),  $[I] = 0.15$  M,  $pH = 7.4$ : DNA/LPEI-2.5 kDa complex ( $\triangle$ ). The lines are guides for the eyes.

between 3 and 5 DNA chains per complex would be compatible with the measured electrical charge and  $R_h$ . These assemblies are reminiscent of small DNA bundles formation induced by trivalent ions [52].

It is surprising that for both polyanions, the observed charge inversion does not occur at  $x = 1$ . Such deviations from stoichiometric association have already been observed [10, 12, 53]. A first explanation might invoke a wrong estimation of the charge ratio  $x$ . The complexation may favor the protonation of PEI [9, 13, 14]. Another explanation involves hydrodynamic effects. As emphasized in ref. [50], the point of vanishing mobility may not coincide with the point of vanishing charge in heterogeneous polyelectrolytes systems. This effect depends on ionic strength and we will come back to this point. If this explanation is relevant, the difference between DNA and PSSNa would then be due to a difference of conformation of the polyelectrolytes chains in the complexes, which leads to different electrophoretic behaviors [51].

We have noticed that the negatively charged complexes below  $x = 0.6$  were slightly aggregated, this is also the case of the positively charged complexes in the decondensation regime above  $x = 1.5$ . Charge inversion favors the dissociation of the complexes, but the decondensation is not complete contrarily to the prediction of the theory. The hydrodynamic radius of the DNA complexes decreases from 185 nm for  $x = 1.5$  to 110 nm for  $x \geq 4.4$ , but remains much larger than the length of bare DNA. In the same  $x$  range, the mobility increases weakly from  $2.1$  to  $2.5 \times 10^{-4} \text{ cm}^2 \text{ V}^{-1} \text{ s}^{-1}$  and the electrophoretic effective charge decreases from  $450e$  to  $330e$ . The same general trends are observed on the PSSNa systems. In that case, the comparison of the apparent hydrodynamics radius of the anionic and cationic complexes with the one of free PSSNa [54] leads to the conclusion that complexes are also already slightly aggregated in the weak complexation

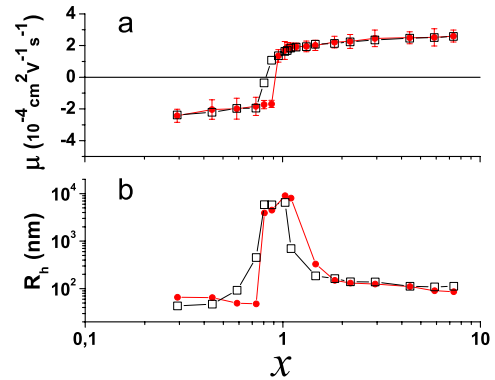


**Fig. 2.** Electrophoretic mobility (a) and hydrodynamics radius (b) plotted as a function of charge ratio  $x$ . DNA concentration  $c = 0.01\%$  ( $w/v$ ),  $[I] = 0.15$  M and  $pH = 7.4$ . DNA/LPEI-2.5 kDa complex ( $\square$ ), DNA/LPEI-25 kDa complex ( $\bullet$ ).

regimes. It appears that the theoretical predictions are confirmed at least qualitatively by the phase diagrams. In the present case, binary complexes with individual polyanions are not observed by DLS. Instead, in this weak complexation regime, small complexes, usually called primary complexes, are observed. The strong complexation regime corresponds to the condensation or secondary aggregation of these primary complexes. It deserves to mention that redissolution of large aggregates is obtained upon addition of a small volume of polyanions stock solutions. Condensed complexes close to the condensation threshold are disassembled into primary complexes by decreasing the charge ratio  $x$ . This important observation indicates that the condensation phenomenon is reversible.

The region of maximum turbidity and hydrodynamic radius corresponds to the domain of existence of the strongly condensed complexes. As the variations of  $R_h$  are continuous, it is difficult to define precisely a threshold of condensation and decondensation and to make a quantitative comparison with the theory of R. Zhang and B. Shklovskii. Note that the largest values of  $R_h$  (above  $6 \mu\text{m}$ ) cannot be trusted because of the limits of the technique of measurement. For DNA, the strong variations of  $R_h$  occur in the range  $0.45 < x < 1.5$ . The theoretical values of the condensation and decondensation threshold,  $x_c$  and  $x_d$  in the presence of salt are given by the following expression [2], which omits unknown numerical factors:

$$x_{c,d} = 1 \mp \frac{1}{\sqrt{\ln(r_s/b)}}. \quad (4)$$

$r_s$  is the Debye screening length and  $b$  the distance between charges assumed to be the same for both polyelectrolytes ( $r_s > b$ ). By taking  $b = 0.17$  nm for DNA and  $r_s = 0.8$  nm for an ionic strength of 0.15 M, one obtains  $x_c = 0.2$  and  $x_d = 1.8$ . The agreement is not bad but may be fortuitous, particularly if one considers the absence of numerical factors in eq. (4).

In order to probe the influence of the translationnal entropy of the chains which is neglected by R. Zhang

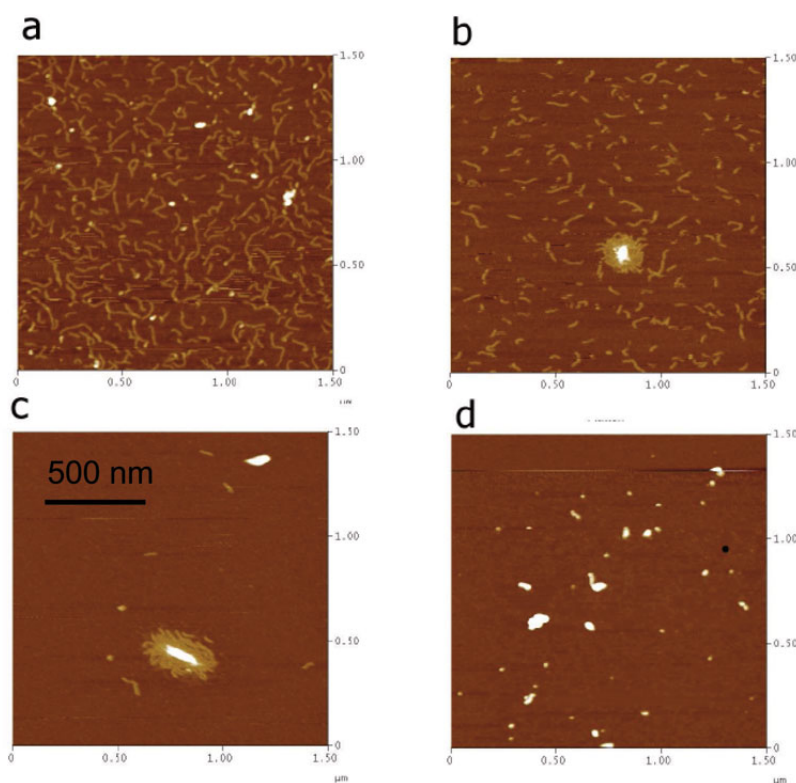


**Fig. 3.** AFM observation of 146 bp-DNA/LPEI-2.5 kDa complexes. The DNA concentration is fixed at 0.01% ( $w/v$ ). Panel (a): DNA fragments alone in solution. Panels (b), (c) and (d) are obtained by increasing LPEI concentration and varying the charge ratio  $x$ ; (b)  $x = 0.6$ , (c)  $x = 1$  and (d)  $x = 5$ . Image size:  $1.5 \mu\text{m} \times 1.5 \mu\text{m}$ . For clarity, vertical profiles are supplied online as supplementary material ([z-profile.pdf](#)).

and B. Shklovskii (and which might explain the relative smoothness of the experimental phase behaviour), we have performed one series of experiments where the concentration of DNA, divided by a factor of 2, is  $c = 0.005\%$  ( $w/v$ ) (fig. 1). We still observe the complexation of LPEI-2.5 kDa with DNA and a charge inversion, but the phenomena of condensation and decondensation are barely noticeable and the dimension of the aggregates remains relatively small even at the maximum of complexation occurring for  $x = 1.1$ , where  $R_h = 255 \text{ nm}$ . The size and the electrophoretic mobility of the complexes for small and large  $x$  are the same as those observed in the preceding experiments and thus appear independent of DNA concentration. Interestingly, the point of charge inversion is shifted from  $x = 0.83$  to  $x = 0.6$ . Again we may incriminate an increased protonation of LPEI by complexation or the mechanisms of electrophoresis.

Another way of probing entropic effects is to vary the molecular weight of the PEI chains. Our observations on the LPEI-25 kDa/146 bp-DNA system are reported in fig. 2 in comparison with those of the LPEI-2.5 kDa-DNA system. At the same monomer concentration, the translational entropy of the 25 kDa chains is 10 times smaller than the one of the 2.5 kDa chains and one expects a more clear-cut phase behaviour with the longer chains. This is indeed the case. The variations of the electrophoretic mo-

bility and hydrodynamic radius as a function of the charge ratio  $x$  are qualitatively the same in both systems but the growth and decrease of the hydrodynamic radius associated to the phenomena of condensation and decondensation are faster with LPEI-25 kDa than with LPEI-2.5 kDa. The charge inversion also occurs more abruptly. Note that the point of zero electrophoretic charge occurs here exactly at  $x = 1$ . One also observes that the values of  $\mu$  and  $R_h$  at small and large  $x$  are the same in both systems. The physics of complexation and charge inversion appears as predicted by theory dominated by electrostatics effects and weakly dependent on molecular details.

*Observations by AFM.* We attempted to observe the structure of the complexes formed by LPEI-2.5 kDa/DNA for different values of the charge ratio  $x$  by Atomic Force Microscopy (fig. 3). Our observations are still qualitative at this stage since the structure of the complexes may be strongly perturbed by adsorption on the mica surface and the drying process, nevertheless the pictures show a well-defined trend. Since the mica is treated with  $\text{MgCl}_2$ , the surface is cationic and will favor the adsorption of anionic species.

We start for reference from the imaging of the DNA 146 bp alone in solution at the same values of concentration and ionic strength as used for the complexes (fig. 3a). The adsorption of the individual DNA fragments

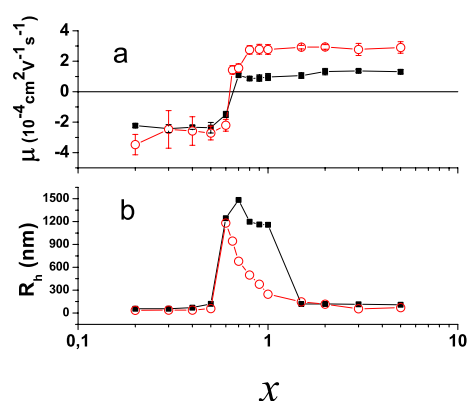


**Fig. 4.** Hydrodynamics radius (a) and electrophoretic mobility (b) of PSSNa/PEI-2.5 kDa plotted as a function of charge ratio  $x$  at a PSSNa concentration  $c = 0.01\%$  ( $w/v$ ) and  $pH = 7.4$ .  $[I] = 0.15$  M ( $\circ$ ),  $[I] = 0.25$  M ( $\blacksquare$ ).

on mica is perfectly visible. For  $x = 0.6$  (fig. 3b), the formation of complexes is characterized by a decrease of the density of adsorbed single DNA chains and the presence of large clusters visible on several pictures, whose size is in the range 50–100 nm. However, it is not possible to distinguish single bare DNA molecules from individual binary complexes. For that reason, the picture may also correspond to the intercomplex disproportionation [2, 3] where condensed and binary complexes coexist. Note that the interactions with the surface may not only favor the adsorption of individual bare or complexed DNA strands, but also promote the dissociation of existing complexes.

For  $x = 1$  (fig. 3c), no free DNA chains or individual binary complexes are present and a few very large clusters settle the surface. This is indeed what we expect in the regime of charge inversion. We have also studied one sample in the cationic regime,  $x = 5$  (fig. 3d). We note the reappearance of numerous relatively small aggregates, which may correspond to partially decondensed cationic complexes. Unlike the other images, the DNA strands are no longer flattened on the surface, but appear as small condensed complexes. This effect might be ascribed to the repulsive interaction between the surface and the complexes. Despite the interactions between the substrate and the polyelectrolytes, which can modify the structure of complexes, there is a nice correlation between the macroscopic phase diagram and the AFM observations. Further work is needed, especially using more reliable imaging methods like AFM at substrate-solution interface or cryomicroscopy.

*Effect of ionic strength.* The ionic strength of the solution plays an important role in the formation of complexes and the effect of addition of a monovalent salt leads to very different behaviors depending on the characteristics and concentrations of the polyelectrolytes [55–57]. R. Zhang and B. Shklovskii have shown theoretically that the domain of existence of condensed complexes becomes broader when the ionic strength is increased. Increasing the ionic strength  $[I]$  indeed decreases the stability of the

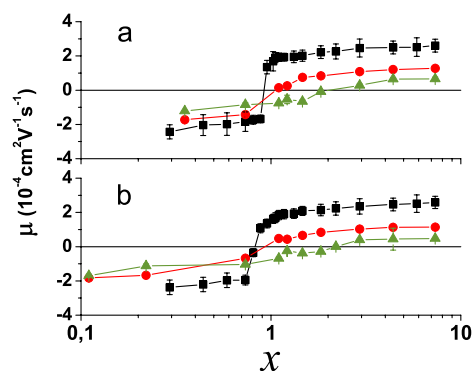


**Fig. 5.** Electrophoretic mobility of DNA/LPEI2.5 kDa complex (a) and DNA/LPEI25 kDa complex (b) as a function of charge ratio  $x$  for different ionic strengths at a DNA concentration  $c = 0.01\%$  ( $w/v$ ) and  $pH = 7.4$ .  $[I] = 0.15$  M ( $\blacksquare$ ),  $[I] = 0.25$  M ( $\bullet$ ) and  $[I] = 0.65$  M ( $\blacktriangle$ ).

systems. We only obtained soluble and stable complexes in the whole  $x$  range at  $[I] = 0.25$  M with the PSSNa/LPEI 2.5 kDa systems (fig. 4).

However, we could perform electrophoretic mobility measurements on unstable slowly precipitating DNA/PEI-25 kDa and DNA/PEI-2.5 kDa complexes at  $[I] = 0.25$  M and  $[I] = 0.65$  M (5). In that case, measurements were also repeated one month after gentle stirring of precipitated complexes. The broadening of the regime of condensation or strong complexation is clearly visible on the measurements of  $R_h$  as a function of  $x$  for the PSSNa system (fig. 4). Salt addition increases the decondensation threshold but does not affect the condensation threshold. A similar observation was made on complexes of DNA and basic proteins in the presence of monovalent salt [7]. This is an effect of the translational entropy of polycations discussed in ref. [3]. Increasing the concentration of polycations favors the condensation of the complexes. In contrast to other polyelectrolyte complexes [55, 57], redissolution of the aggregates at high ionic strength is not observed.

The broadening of the inversion region is also observable in the DNA assemblies (fig. 5). One observes a spectacular drift of the point of charge inversion for  $[I] = 0.65$  M, occurring at  $x = 2$ . This indicates that part of the polycations remain free in solution. In this regime the short-range attractive electrostatic correlations, which govern complexation, start to be screened. Similar effects of salt on overcharged glass surfaces [58] or spermine/DNA complexes [8] have recently been reported. Note that the shift of the isoelectric point is independent of the polycation molecular weight.

*Structure of the complexes determined by SANS.* The systems described above are too dilute to be studied by neutron scattering. We thus looked for stable complexes with a larger polyanion concentration, 0.2% ( $w/v$ ). Unfortunately, the only soluble and stable complexes that we could obtain were anionic with a small charge ratios

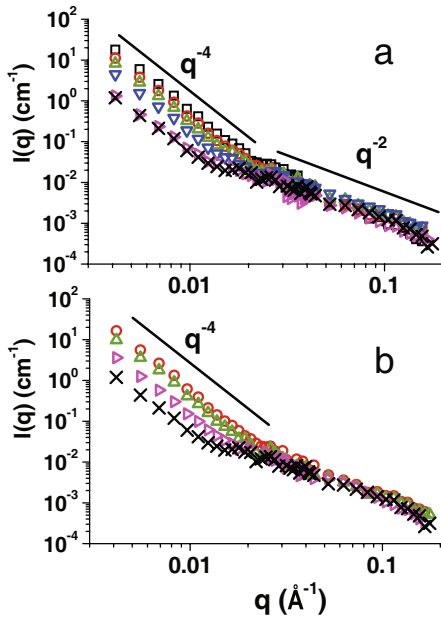


**Fig. 6.** Intensity scattered by LPEI-2.5 kDa/DNA complexes (a) and LPEI-25 kDa/DNA complexes (b) for different charge ratios  $x$  (DNA concentration  $c = 0.2\%$  ( $w/v$ ),  $[I] = 0.15$  M,  $pH = 7.4$ ):  $x = 0.022$  ( $\blacktriangleright$ ),  $x = 0.055$  ( $\blacktriangledown$ ),  $x = 0.11$  ( $\blacktriangle$ ),  $x = 0.22$  ( $\circ$ ),  $x = 0.36$  ( $\square$ ). Intensity scattered by free DNA in solution ( $\times$ ). The straight lines represent the power law dependence of the intensity.

ranging from  $x = 0.022$  to  $0.37$  and the same negative electrophoretic mobility,  $\mu = -2.2 \pm 0.1 \cdot 10^4 \text{ cm}^2 \text{ V}^{-1} \text{ s}^{-1}$ .

The intensity scattered by DNA and PSSNa alone at  $c = 0.2\%$  ( $w/v$ ) and  $[I] = 0.15$  M, shown in figs. 6 and 7, presents similar features. The intensity scattered by DNA and that one observed with 400 bp DNA at a slightly higher concentration and similar salt concentration [42] resemble each other greatly. Two scattering vector domains can be distinguished for both polyanion spectra. At low  $q$  ( $q < 0.01 \text{ \AA}^{-1}$ ), an upturn of the intensity is observed. Although still debated, this phenomenon is usually ascribed to the existence of domains of higher polymer density associated to fluctuations of concentration [42, 59–61]. This upturn domain has been reported for flexible (PSSNa [60]) or rigid polyanions (DNA [42]) as well. It deserves to be mentioned that in both cases, no local maximum usually assigned to repulsive electrostatic interactions is observed. Even at this increased polymer concentration, the ionic strength is sufficiently high to screen repulsive electrostatic interactions [42, 62].

At large  $q$  ( $q > 0.01 \text{ \AA}^{-1}$ ), the intensities decays show a power law dependence ( $I(q) \propto q^{-\alpha}$ ). The asymptotic intensity scattered by PSSNa ( $\alpha = 1.26 \pm 0.07$ ) reveals the stretching of the polyanion. The expected value of the exponent for long rodlike DNA molecules is  $\alpha \simeq 1$ . Due to the finite length, asymptotic behavior of short DNA fragments depends on the molecular weight and the ionic strength [42, 63]. For instance, it has been reported that for a 400 bp DNA fragment, the exponent value increases

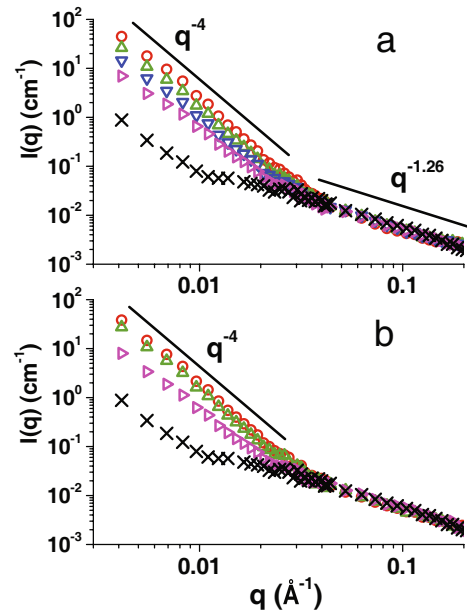


**Fig. 7.** Intensity scattered by LPEI-2.5 kDa/PSSNa (a) and LPEI-25 kDa/PSSNa complexes (b) for different charge ratios  $x$  (PSSNa concentration  $c = 0.2\%$  ( $w/v$ ),  $[I] = 0.15$  M,  $pH = 7.4$ ):  $x = 0.022$  ( $\blacktriangleright$ ),  $x = 0.055$  ( $\blacktriangledown$ ),  $x = 0.11$  ( $\blacktriangle$ ),  $x = 0.22$  ( $\circ$ ). Intensity scattered by free PSSNa in solution ( $\times$ ). The straight lines represent the power law dependence of the intensity.

with ionic strength within the range  $1 < \alpha < 2$  [42]. For the 146 bp DNA at a ionic strength  $[I] = 0.15$  M, we obtain  $\alpha = 2.0 \pm 0.1$ . The cross-section radius of gyration  $R_c$  of DNA can be determined using the asymptotic behavior of  $I(q)$  at high  $q$ . For a rigid cylinder, the expression of the scattered intensity at high  $q$  is [42, 64]

$$I(q) = \frac{I_0}{q} e^{-\frac{q^2 R_c^2}{2}}. \quad (5)$$

The fit of the data for  $q > 0.05 \text{ \AA}^{-1}$  yields an estimate for the cross-section of DNA  $R_c = 8.9 \pm 0.6 \text{ \AA}$ . This value is slightly lower than those reported by SANS and SAXS studies of short DNA molecules [42, 64] ( $R_c = 10.05 \text{ \AA}$ ).

When mixed with PEI-2.5 kDa at low charge ratio  $x = 0.022$ , the intensity scattered by the complex (fig. 6) is identical to that of free DNA, indicating that the complexation is weak in this case. The scattering appears mainly due to DNA because the chains are not associated and the contrast between PEI and  $D_2O$  is smaller than that of DNA. When the charge ratio  $x$  is further increased by adding PEI molecules, the scattering intensity increases strongly at small angles, showing complex formation. Large condensed aggregates are observed for  $x = 0.22$  and  $x = 0.36$ . This is not surprising since these values are beyond the predicted condensation threshold [2] for this ionic strength. However the observation of smaller but condensed complexes for  $x = 0.11$  and  $x = 0.055$  are not predicted by theory, since binary complexes are instead expected. This discrepancy might be due to ionic

strength effects enhanced at high concentration as described in [2].

The intensity decay in the small- $q$  regime exhibits a  $q^{-4}$  Porod behavior characteristic of dense aggregates with a sharp interface. In the high- $q$  domain ( $3 \cdot 10^{-2} \text{ \AA}^{-1} < q < 2 \cdot 10^{-1} \text{ \AA}^{-1}$ ) the intensity scattered by the complexes is identical to that scattered by free DNA. The rodlike structure of DNA is not affected by complexation. We note that the spectra do not exhibit diffraction peaks at large angle contrary to what is observed on precipitated complexes (data not shown) [65]. In our case, there is no local hexagonal ordering of the DNA molecules. Scattered intensities by complexes made of higher molecular weight PEI-25 kDa present the same features, indicating that the molecular weight of the polycation has no influence on the structure of anionic complexes. Contrary to what is observed with short PEI molecules, aggregation already appears for the lowest  $x = 0.022$  and the higher charge ratio  $x = 0.22$  complex is unstable.

The intensities scattered by the PSSNa-LPEI complexes as a function of the charge ratio are shown in fig. 7. No weak aggregation is observed and the shape of the spectra as the charge ratio increases is surprisingly very similar to that observed with DNA. The local stretched structure of the polyanion is not modified by complexation and large complexes of increasing size are observed as  $x$  increases. Again, the  $q^{-4}$  scattered intensity decay in the low- $q$  range shows that the polyanion aggregates under the form of large assemblies with a sharp interface. The structure of the polyanion differs from the one observed with pH-sensitive weak polyelectrolyte complexes where the chains condense into homogeneous spheres [14].

## 4 Conclusions

Our comparative study of the different LPEI/DNA and LPEI/PSSNa systems shows that the phase diagrams of the two systems are very similar. This similarity evidences that the complexation process does not depend on the structure and rigidity of the polyanion, nor on the length of the polycations, but is mainly controlled by the electrostatic interactions, in agreement with recent theories, which also correctly predict the observed sequence of weak complexation, strong complexation, charge inversion and decondensation as the charge ratio of the complexes increases, as well as the effects of ionic strength. These results complete and prolongate similar observations obtained on other systems of complexes, involving multivalent ions or small polymer chains [7]. We have obtained stable DNA-LPEI complexes in the whole range of the charge ratio  $x$  which may have interesting applications in gene therapy. For that purpose, it is necessary to invert the charge of DNA in order to facilitate the merging of the complex with negatively charged cell membranes. Further studies on the reversibility of complexation on the entire phase diagram coupled with dynamical information using selective methods of investigation like NMR should help us in studying the thermodynamical equilibrium of the

complexes. An effort has to be made for studying in detail the structure of dilute individual complexes, in the anionic and cationic (overcharged) range. We have shown that AFM and scattering techniques are useful tools to reach this goal. A certain ambiguity remains concerning the interpretation of the electrophoresis experiments performed on the complexes, a better knowledge of the charge of the complexes and of the distribution of the charges in the complexes would be very useful.

We thank the Laboratoire Léon Brillouin (CEA-Saclay) for allocation of neutron beam time, Madalena Renouard for her help during DNA extraction operation, Françoise Livolant for useful discussions and Philippe Roger for the access to his Zetameter. V. Mengarelli acknowledges the receipt of a Marie Curie Actions Grant, Contract N° MEST-CT-2004-514307.

## References

1. T. Nguyen, I. Rouzina, B.I. Shklovskii, *J. Chem. Phys.* **112**, 2562 (2000).
2. R. Zhang, B. Shklovskii, *Physica A* **352**, 216 (2005).
3. R. Zhang, B. Shklovskii, arXiv:cond-mat/0408153v3 (2005).
4. S.Y. Park, R.F. Bruinsma, W. Gelbart, *Europhys. Lett.* **46**, 454 (1999).
5. A.Y. Grosberg, T.T. Nguyen, B.I. Shklovskii, *Rev. Mod. Phys.* **74**, 329 (2002).
6. T.T. Nuyen, B. Shklovskii, *Phys. Rev. Lett.* **89**, 018101 (2002).
7. E. Raspaud, J. Pelta, M. de Frutos, F. Livolant, *Phys. Rev. Lett.* **97**, 068103 (2006).
8. K. Besteman, K.V. Eijk, S.G. Lemay, *Nat. Phys.* **3**, 641 (2007).
9. A. Kabanov, V. Kabanov, *Bioconjugate Chem.* **6**, 7 (1995).
10. G. Petzold, A. Nebel, H.M. Buchhammer, K. Lunikwitz, *Colloid Polym. Sci.* **276**, 125 (1998).
11. H.M. Buchhammer, G. Petzold, K. Lunikwitz, *Langmuir* **15**, 4306 (1999).
12. J. Kekkonen, H. Lattu, P. Stenius, *J. Colloid Interface Sci.* **234**, 384 (2001).
13. S. Choosakoonkriang, B. Lobo, G. Koe, J. Koe, C. Mid-daugh, *J. Pharm. Sci.* **92**, 1710 (2003).
14. V. Mengarelli, L. Auvray, M. Zeghal, *Europhys. Lett.* **85**, 58001 (2009).
15. V. Mengarelli, L. Auvray, D. Clemens, M. Zeghal, *Phys. Rev. E* **84**, 021805 (2011).
16. D. Störkle, S. Duschner, N. Heimann, M. Maskos, M. Schmidt, *Macromolecules* **40**, 7998 (2007).
17. V. Kabanov, V. Sergeev, O. Pyshkina, A. Zinchenko, A. Zezin, J. Joosten, J. Brackman, K. Yoshikawa, *Macromolecules* **33**, 9587 (2000).
18. H. Walker, S. Grant, *Colloid. Surf. A* **119**, 229 (1996).
19. K. Keren, Y. Soen, G.B. Yoseph, R. Gilad, E. Braun, U. Sivan, Y. Talmon, *Phys. Rev. Lett.* **89**, 088103 (2002).
20. I. Gössl, L. Shu, A.D. Schlüter, J. Rabe, *J. Am. Chem. Soc.* **124**, 6860 (2002).
21. Y. Wang, K. Kimura, Q. Huang, P.L. Dubin, W. Jaeger, *Macromolecules* **32**, 7128 (1999).
22. G. Decher, *Science* **277**, 1232 (1997).

23. J.B. Schlenoff, *Langmuir* **25**, 14007 (2009).
24. O. Boussif, F. Lezoualc'h, M. Zanta, M. Mergny, D. Scherman, B. Demeneix, J. Behr, *Proc. Natl. Acad. Sci. U.S.A.* **92**, 7297 (1995).
25. K. Kunath, A. von Harpe, D. Fischer, H. Petersen, U. Bickel, K. Voigt, T. Kissel, *Journal Controll. Release* **89**, 113 (2003).
26. S. de Smedt, J. Demeester, W. Hennink, *Pharm. Res.* **17**, 113 (2000).
27. A. Kudlay, A. Ermoshkin, M.O. de la Cruz, *Macromolecules* **37**, 9231 (2004).
28. M. Castelnovo, J.F. Joanny, *Eur. Phys. J. E* **6**, 377 (2001).
29. Z. Ou, M. Muthukumar, *J. Chem. Phys.* **124**, 154902 (2006).
30. R. Winkler, M. Steinhauser, P. Reineker, *Phys. Rev. E* **66**, 021802 (2002).
31. Y. Hayashi, M. Ullner, P. Linse, *J. Phys. Chem. B* **107**, 8198 (2003).
32. J. Lee, Y.O. Popov, G.H. Fredrickson, *J. Chem. Phys.* **128**, 224908 (2008).
33. S. Lee, T.T. Le, T.T. Nguyen, *Phys. Rev. Lett.* **105**, 248101 (2010).
34. C.B. Bucur, Z. Sui, J.B. Schlenoff, *J. Am. Chem. Soc.* **128**, 13690 (2006).
35. K. Yoshikawa, M. Takahashi, V.V. Vasilevskaya, A.R. Khokhlov, *Phys. Rev. Lett.* **76**, 3029 (1996).
36. D. Dunlap, A. Maggi, M. Soria, L. Monaco, *Nucleic Acids Res.* **25**, 3095 (1997).
37. E. Raspaud, M.O. de la Cruz and J.-L. Sikorav, F. Livolant, *Biophys. J.* **74**, 381 (1998).
38. C. Cooper, P. Dubin, A. Kayitmazer, S. Turksen, *Curr. Opin. Colloid Interface Sci.* **10**, 52 (2005).
39. J.L. Sikorav, J. Pelta, F. Livolant, *Biophys. J.* **67**, 1387 (1994).
40. D. Yankov, R. Stateva, J. Trusler, G. Cholakov, *J. Chem. Engin. Data* **51**, 1056 (2006).
41. B. Chu, *Laser Light Scattering*, 2nd edition (Academic Press, New York, 1990).
42. R.P. R. Borsali, H. Nguyen, *Macromolecules* **31**, 1548 (1998).
43. J.G. de la Torre, S. Navarro, M.L. Martinez, *Biophys. J.* **66**, 1573 (1994).
44. D.A. Hoagland, E. Arvanitidiou, C. Welch, *Macromolecules* **32**, 6180 (1999).
45. M. Muthukumar, *Electrophoresis* **17**, 1167 (1996).
46. N. Stellwagen, C. Gelfi, P. Righetti, *Biopolymers* **42**, 687 (1997).
47. L. Hamon, D. Pastré, P. Dupaigne, C.L. Breton, E.L. Cam, O. Pietrement, *Nucl. Acids Res.* **35**, No. 8 e58 (2007) doi:10.1093/nar/gkm147.
48. P. Wissenburg, T. Odijk, P. Cirkel, M. Mandel, *Macromolecules* **28**, 2315 (1995).
49. E. Stellwagen, N. Stellwagen, *Electrophoresis* **23**, 2794 (2002).
50. D. Long, A.V. Dobrynin, M. Rubinstein, A. Ajdari, *J. Chem. Phys.* **108**, 1234 (1998).
51. D. Long, J.L. Viovy, A. Ajdari, *Phys. Rev. Lett.* **76**, 3858 (1996).
52. M. Mandelkern, N. Dattagupta, D. Crothers, *Proc. Natl. Acad. Sci. U.S.A.* **78**, 4294 (1981).
53. H.M. Buchhammer, G. Kramer, K. Lunikwitz, *Colloid. Surf. A* **95**, 299 (1994).
54. N. Lin, W. Deen, *J. Colloid Interface Sci.* **153**, 483 (1992).
55. H. Dautzenberg, N. Karibyants, *Macromol. Chem. Phys.* **200**, 118 (1999).
56. A. Thünemann, M. Müller, H. Dautzenberg, J.F. Joanny, H. Löwen, *Polyelectrolyte complexes*, Vol. **166** *Advances in Polymer Science* (Springer, Berlin, 2004).
57. T. Andersson, S. Holappa, V. Aseyev, H. Tenhu, *Biomacromolecules* **7**, 3229 (2006).
58. F.H.J. van der Heyden, D. Stein, K. Besteman, S.G. Lemay, C. Dekker, *Phys. Rev. Lett.* **96**, 224502 (2006).
59. M. Nierlich, C. Williams, F. Boué, J. Cotton, M. Daoud, B. Famoux, G. Jannink, C. Picot, M. Moan, C. Wolff *et al.*, *J. Phys. (Paris)* **40**, 701 (1979).
60. H. Matsuoka, D. Schwahn, N. Ise, *Macromolecules* **24**, 4227 (1991).
61. J.H.E. Hone, A.M. Howe, T. Cosgrove, *Macromolecules* **33**, 1206 (2000).
62. L. Wang, V. Bloomfield, *Macromolecules* **24**, 5791 (1991).
63. J. Puigdomenech, L. Perez-Grau, J. Porta, M. Vega, P. Sicre, M. Koch, *Biopolymers* **28**, 1505 (1989).
64. M. Koch, Z. Sayers, P. Sicre, D. Svergun, *Macromolecules* **28**, 4904 (1995).
65. J. DeRouchey, R.R. Netz, J.O. Rädler, *Eur. Phys. J. E* **16**, 17 (2005).